

## **HIBERNIA THREE-PHASE RELATIVE PERMEABILITY MEASUREMENTS AT RESERVOIR CONDITIONS**

By Daniel R. Maloney and Brad E. Milligan, ExxonMobil Upstream Research Company

*This paper was prepared for presentation at the International Symposium of the Society of Core Analysts held in Vienna, Austria, 27 August – 1 September 2017*

### **ABSTRACT**

The purpose of this study was to provide three-phase relative permeability versus saturation data to support investigation of double-displacement process (DDP) and water-alternating-gas (WAG) schemes for the Hibernia Field in East Canada. Goals were to measure three-phase steady-state relative permeabilities, gain description of hysteresis during WAG, and to reduce uncertainty of three-phase trapped gas saturation magnitude. Innovative aspects include the design of saturation trajectories to mimic saturation changes during DDP and WAG, and measurement of three-phase steady-state relative permeabilities at saturation conditions along those trajectories using live fluids and reservoir conditions.

Hibernia core plugs of this study were the same used in a previous study.<sup>1</sup> The plugs were previously characterized as oil-wet. The reservoir-condition DDP test of that study began with live brine and live oil injection at a ratio of 9:1 until a steady-state condition was established, then continued by flooding with pre-equilibrated gas until residual oil saturation was achieved. Results described a saturation path or trajectory during DDP. In this work, two-phase steady-state gas-oil and oil-brine relative permeability tests were performed to confirm agreement with previous measurements. Gas-brine relative permeability tests were also performed. For three-phase testing, the fluid injection sequence was designed to approximate the same saturation path or trajectory as that of the previous DDP test. At specific saturations along that trajectory, three-phase relative permeabilities were measured under steady-state conditions. After finishing the double displacement trajectory, steady-state testing continued with gas and brine injection representing several cycles of water-alternating-gas. Measurements from additional saturation trajectories provided good coverage of the three-phase saturation envelope.

Under conditions of three-phase flow, for this oil-wet rock, the gas phase exhibited the greatest amount of saturation-history-dependent hysteresis. The two-phase gas-brine curves, in addition to gas-oil curves, were found to be useful for understanding when and why either brine or oil had the greatest influence on three-phase gas relative permeabilities. The process of following a specific saturation trajectory for three-phase testing provided an efficient means for completing the three-phase tests in a relatively short time period (3.5 months). This protocol of performing relatively quick displacements (gas flood after waterflood or waterflood after gas flood) is recommended to identify saturation paths to follow during subsequent three-phase steady-state flow tests.

## INTRODUCTION

Measurements of this project relate to the Hibernia Field, which is located 300 km southeast of St. John's Newfoundland and Labrador, Canada in the Jeanne D'Arc Basin. It is 250 km offshore with 80 m water depth. A concept being considered is gas flooding some of the Hibernia Formation waterflood blocks when secondary recovery is complete. Screening calculations and field experience with gas injection in the northern fault blocks indicate that WAG injection in blocks currently undergoing waterflood has potential to yield additional oil recovery.<sup>2</sup> Objectives of SCAL studies are to provide the most representative three-phase relative permeability curves for pilot and full-field studies, to investigate WAG three-phase hysteresis effects, and to assist in the estimation of recovery efficiency.<sup>2</sup>

In 2006, Wang *et al.*<sup>1</sup> reported results from gas injection following a waterflood on core plugs from the Hibernia B-16-17 well in the V-Block. During the experiment, gas injection began after the foot-long composite core was flooded at a 9:1 water-oil injection ratio. The authors describe that some evaporation of water and oil may have occurred during the test. They made corrections to account for the loss. The blue "target" trend on Figure 5 shows the saturation path or trajectory that resulted during the double-displacement test, after saturations were corrected for fluid loss because of evaporation. This trend shows that, during the early stage of the gas flood, mostly brine was produced until brine saturation (fraction of pore volume) decreased to about 0.35. Thereafter, injected gas displaced mostly oil until oil saturation was reduced to about 0.10.

Data from the 2006 investigation<sup>1</sup> left some uncertainty in relative permeability curves, because three-phase relative permeabilities were calculated using a modification of the JBN<sup>3</sup> unsteady-state method, and because of questions related to "evaporation" losses. To reduce uncertainty, additional testing was warranted. The additional tests are the subject of this paper.

## TEST METHODS AND DESCRIPTIONS

### Fluids and Conditions

Brine was of the same Hibernia recipe used in the previous investigation. The brine composition, as well as various other rock and fluid properties (USBM wettability index, capillary pressure curves, two-phase relative permeability curves, interfacial tensions, and pore size distribution) can be found in ref. 1. Live Hibernia oil and equilibrium gas were used for reservoir-condition steady-state gas-oil, oil-brine, and brine-oil-gas tests. Synthetic solution gas was prepared and recombined with stock tank oil to match the reservoir fluid composition. Bubble point at 213 °F was 3241 psig. Table 1 provides descriptions of fluids, test conditions, and viscosities of fluids used in tests of this project. Viscosities listed in the table are those measured during flow tests after fluids were equilibrated.

For wettability restoration, within confining pressure cells, plugs were centrifuged at 3200 rpm (120 psi capillary pressure) in gas-displacing-brine mode to initial brine saturation, flooded with degassed or “dead” Hibernia oil to displace gas, and aged 6 weeks at 213°F.

Test Type	Fluids	T, °F	Pore pressure, psig	Net confining pressure, psi	$\mu_w$ , cP	$\mu_o$ , cP	$\mu_g$ , cP
g-w	nitrogen, brine	120	1000	4000	0.915	**	0.020
g-o	live gas, live oil	213	3241	4000	**	0.793	0.031
o-w	live oil, live brine	213	3241	4000	0.411	0.793	**
w-o-g	live brine, live oil, live gas	213	3241	4000	0.411	0.793	0.031

### Core Plugs

Core plugs were the same plugs used for an earlier double-displacement experiment.<sup>1</sup> Plugs were stacked to build a composite with the same arrangement as in the earlier investigation, and loaded into a coreholder. With 4000 psi net confining pressure, permeability of the composite to gas (nitrogen) was 2045 mD, whereas the harmonic average from individual plug properties was 2052 mD. Permeability of the composite to brine was 2200 mD, compared to the harmonic average of 2051 mD from individual plug properties. When arranged in a composite,  $k_w$  was slightly greater than  $k_g$ . This was also observed in the prior investigation (see Table 2, ref. 1). The reason for this difference has not been resolved. At the beginning of the gas-oil test, oil permeability was 1514.8 mD at residual water saturation ( $S_{wirr} = 0.042$ ). This permeability value (1514.8 mD) was used as the basis for normalizing all permeabilities to express results as relative permeabilities.

### Flow Apparatus

The flow apparatus is depicted in Figure 1. All components are mounted within a temperature-controlled environment. The apparatus is a “closed-loop” recirculating system. Compared to a “single-pass” system, fluid volume requirements are less, fluids are better equilibrated, and experimental anomalies such as mass transfer and evaporation losses are reduced or eliminated.

At upstream and downstream locations with respect to the composite sample, pressures  $P_1$  and  $P_2$  are measured by high accuracy quartz transducers. Quizix pumps are used for fluid injection. The pumps refill by drawing fluids from the three-phase acoustic separator. A servo pump maintains downstream pressure constant by pushing gas into or withdrawing gas from the separator. Saturation changes within the composite are determined continuously during a test by volumetric balance. Increases and decreases in brine, oil, and gas volumes within the composite are reflected by corresponding changes in fluid volumes within the separator, pumps, and tubing. By knowing the volumetric contents of the separator, pumps, and tubing at all times, saturations within the composite are determined. After finishing a test, volumes of fluids extracted from the composite confirmed results from volumetric balance. Additional descriptions are available elsewhere.<sup>4, 5</sup>

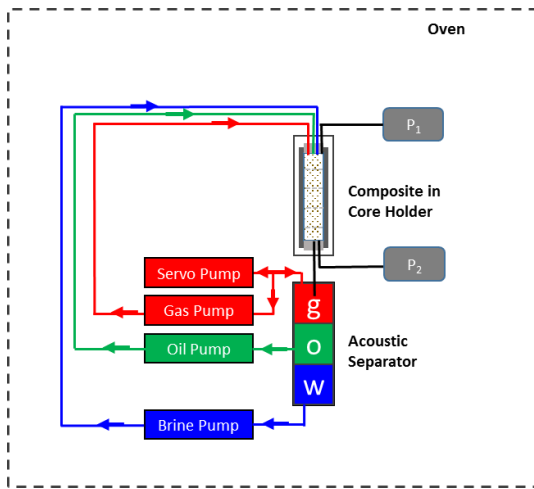


Figure 1 Simple schematic of the steady-state relative permeability apparatus.

### Permeability and Relative Permeability Equations

Steady-state permeabilities were calculated using the Darcy equation. For gas,

$$k_g = 2 P_1 Q_{g1} \mu_g L / [A(P_1^2 - P_2^2)] \quad (1)$$

where  $k_g$  is permeability to gas,  $Q_{g1}$  is the upstream gas injection rate or delivery rate of the gas pump when injecting gas into the composite,  $\mu_g$  is viscosity of the gas (which is approximated as a constant over the pressure range from  $P_1$  to  $P_2$  for these experiments),  $L$  is length of the composite,  $A$  is cross sectional area of the composite,  $P_1$  is upstream pressure, and  $P_2$  is downstream pressure. (“Pressure drop” equals  $P_1$  minus  $P_2$ .)

For the liquid phases, at steady-state, flow rates and viscosities are assumed constant throughout the sample over the pressure range from  $P_1$  to  $P_2$ . Thus, brine permeability is calculated from

$$k_w = Q_{w1} \mu_w L / [A(P_1 - P_2)], \quad (2)$$

and oil permeability is calculated from

$$k_o = Q_{o1} \mu_o L / [A(P_1 - P_2)]. \quad (3)$$

To express results as relative permeabilities, effective permeabilities are normalized by dividing by a common basis. For this work, the basis was  $k_o$  at  $S_{wirr}$ .

### Data Labels and Saturation History Description

In sections that follow, saturations are expressed as fractions of pore volume, with brine, oil, and gas saturations abbreviated as  $S_w$ ,  $S_o$ , and  $S_g$ . Relative permeabilities are represented by  $k_r$  followed by a letter representing the fluid of interest; for example,  $k_{rw}$  means brine relative permeability.

The convention used in this document is to label data sets with direction of saturation change of brine, oil, and gas sequentially, using letter “D” for decreasing, “I” for

increasing, “R” when the phase is at or near residual saturation and is not being injected, and “Ø” when the phase is absent. A number associated with each “D” or “I” indicates the number of cycles of decreasing or increasing saturation that the fluid phase has experienced. The same convention is used for labeling two- and three-phase data to facilitate comparison. For example, with residual brine saturation present, a first displacement of oil by gas is (R, D1, I1). The first cycle of water displacing oil beginning at  $S_{wirr}$  without gas present in the pore system is (I1, D1, Ø), and if followed by gas injection to displace oil and brine, continues as (D2, D1, I1).

### **Two-Phase Steady-State Tests**

Gas-Brine – A gas-brine steady-state test was performed, beginning with a measure of  $k_w$  at  $S_w=1$  followed by gas-displacing-water (D1, Ø, I1) and water-displacing-gas (I1, Ø, D1). After the test, the composite was cleaned. The test was run again as a consistency check.

Gas-Oil with  $S_{wirr}$  Present – Steady-state relative permeability testing included measurements in cycles of oil saturation decreasing (R, D1, I1) and then increasing (R, I1, D1). The last step of the sequence was an oil flood and compress-back to put gas back into solution.

Oil-Brine – Beginning with  $S_{wirr}$ , oil-brine relative permeabilities were measured in steps of increasing brine saturation (I1, D1, Ø) to the launch point for three-phase flow.

### **Three Phase Steady-State Tests**

Once steady-state is achieved at a particular saturation condition, the process of measuring two- and three-phase relative permeabilities is similar in that permeabilities are calculated from rates and pressure drops, permeabilities are divided by the basis to yield relative permeabilities, and average saturation is quantified using the acoustic separator. In a two-phase test, controlling the direction of saturation change is straightforward: implement a sequence of increasing or sequence of decreasing fractional flows. Controlling direction of saturation change with three flowing phases is more challenging; the direction of saturation change depends on rates of three fluid phases and the saturation history. The sequence of flow rate adjustments during a three-phase test is important for following a defined saturation path.

The first three-phase trajectory was designed to approximate saturation history during the previous double-displacement test.<sup>1</sup> It was important not to stray off path, because the first trajectory would be most representative and least affected by prior three-phase saturation history. Target saturations were selected in sequence along the trajectory. The challenge was to develop a schedule of brine, oil, and gas injection rates to pilot along the desired saturation trajectory without unintended saturation reversals or excessive pressure drops. The approach taken was to first graph results from the two-phase tests as phase relative permeability versus phase saturation to identify trends. The  $k_{ro}$  versus  $S_o$  plot showed that oil relative permeability was essentially a function of oil saturation, so a fit to all of the two-phase  $k_{ro}$  versus  $S_o$  data was used to estimate  $k_{ro}$  for a given target oil saturation

condition. From the plot of  $k_{rw}$  versus  $S_w$  using two phase data, the relative lack of hysteresis from the gas-water test attracted the use of the gas-water trend to predict  $k_{rw}$  from  $S_w$ . In retrospect, a better predictor would have been to use the trend from the (D2, I2,  $\emptyset$ ) oil-brine cycle. There was enough variability in  $k_{rg}$  versus  $S_g$  that the arbitrary choice was to use a trend from the combined gas-water (I1,  $\emptyset$ , D1) and gas-oil ( $\emptyset$ , I1, D1) data to predict  $k_{rg}$  from  $S_g$ . These trends were then used to predict relative permeabilities for each target saturation along the trajectory. Relative permeabilities were multiplied by the basis of normalization to yield permeabilities. Finally, for a given pressure drop, flow rates (brine, oil, and gas) were calculated from permeabilities. This approach was not perfect, but was found to be adequate.

During the first saturation trajectory, after approaching residual oil saturation with three-phase flow, oil injection was stopped and cycles of increasing and decreasing brine and gas saturations were imposed. Thereafter, three phase flow was reinitiated to trace a path back toward a residual brine saturation condition. The last step of the sequence was to flood with oil at elevated pore pressure in an attempt to put gas back into solution to prepare for additional saturation trajectories.

For labeling purposes, after finishing a trajectory and compressing to put gas back into solution, it was assumed that the next trajectory would start over on the (I1, D1,  $\emptyset$ ) cycle.

Two additional three-phase saturation trajectories were performed, beginning with higher  $S_w$  condition. The final saturation trajectory was a constant-rate waterflood to  $S_{or}$ , from which relative permeabilities were calculated by the Jones-Roselle graphical method.<sup>6</sup>

## RESULTS

From the entire data set, highest injection rates for brine, oil, and gas were 8.7 cm<sup>3</sup>/min, 8 cm<sup>3</sup>/min, and 83 cm<sup>3</sup>/min respectively. The highest recorded pressure drop was 31 psi.

### Two Phase

Two-phase data trends were fitted with Corey functions. These Corey functions are shown on graphs of two-phase and three-phase relative permeability results. For two-phase measurements, saturations are estimated to be accurate to within 0.03 saturation units. For three-phase flow, saturations are estimated to be accurate to within 0.04 saturation units.

Gas-Brine - Results from two tests (a, b) on the same composite are shown in Figure 2. Residual brine saturation at the end of (D1,  $\emptyset$ , I1) in test (a) was 0.23 compared to the value of 0.15 from test (b). These results were achieved by gas flooding, which does not provide enough drainage capillary pressure to achieve irreducible brine saturation. In this case, even though residual brine saturation from test (a) was greater than that from test (b), results from both tests are comparable. Without oil in the pore system, there is little if any cycle-dependent hysteresis in brine phase relative permeability versus brine saturation, whereas I1 and D1 curves are quite different for the gas phase.

Gas-Oil - Results from gas-oil steady-state relative permeability versus saturation measurements are shown in Figure 3. The oil and gas relative permeability curves show little if any hysteresis.

Oil-Brine - Two-phase brine-displacing-oil steady-state relative permeabilities (I1, D1,  $\emptyset$ ) were measured only to the saturation state at which three-phase flow was initiated (Trajectory 1). After the fourth steady-state (I1, D1,  $\emptyset$ ) measurement with  $S_w = 0.25$ , a valve error briefly caused  $S_w$  to increase to about 0.55 before the issue was identified and corrected. After correction, the next two (I1, D1,  $\emptyset$ ) brine relative permeabilities with brine saturations of 0.41 and 0.46 respectively follow the (D2, I2,  $\emptyset$ ) Corey trend (Fig. 4 and 6).

Figure 4 compares this limited data with results from Ref. 1, Figure 11. Reference 1 data is denoted “2005” in the figure legend.

Another two-phase oil-brine data set was obtained in this investigation as a fourth saturation trajectory after all other measurements were completed. Prior to the fourth trajectory, the composite had undergone multiple cycles of increasing and decreasing brine, oil, and gas saturations, finishing with an oil-flood to residual brine saturation and compress-back that put gas back into solution. Trajectory 4 consisted of a constant-rate waterflood from which relative permeabilities were calculated by the Jones-Rozelle method.<sup>6</sup> As shown in Figure 4, the unsteady-state results, labeled as (Ix, Dx,  $\emptyset$ ) with cycle number denoted “x” to indicate many cycles of increasing and decreasing saturation, are in reasonable agreement with (D2, I2,  $\emptyset$ ) trends from steady-state measurements. Although it was a brine-saturation-increasing test, the brine relative permeability data follows the D2 trend. Apparently, when the system contains oil, after the first cycle of increasing brine saturation, brine relative permeabilities from subsequent decreasing and increasing brine saturation cycles follow the D2 trend. The figure shows little if any cycle-dependent hysteresis in oil-phase relative permeability versus saturation.

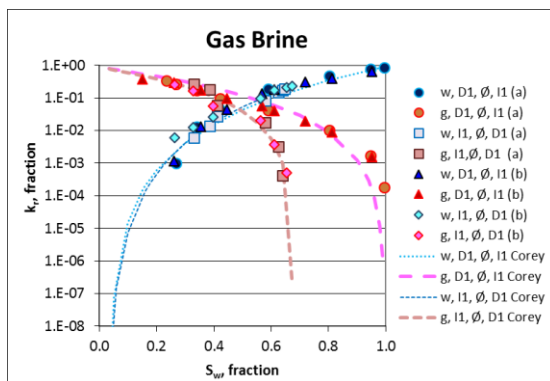


Figure 2 Gas-brine  $k_r$  (2 tests) and Corey fits.

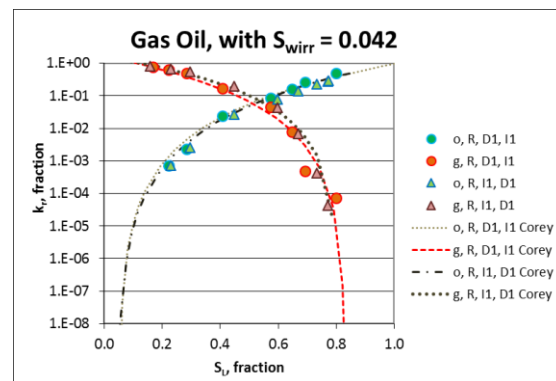


Figure 3 Gas-oil  $k_r$  (with  $S_{wi}$ ) and Corey fits.

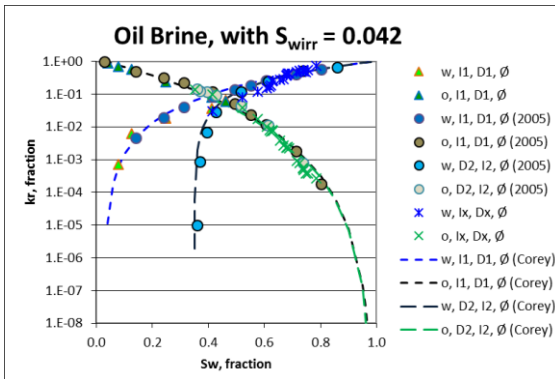


Figure 4 Oil-brine  $k_r$  and Corey fits.

### Three Phase

Trajectory 1 – Figure 5 shows saturations at which relative permeabilities were measured during Trajectory 1. The trajectory was close to that of the Target path. On this type of plot, saturation (fraction of pore volume) equals one for the phase of interest at the apex and zero at the opposite side of the triangle. Lines between the apex and opposite side are in 0.1 saturation fraction increments.

The last sequence of Trajectory 1 was to oil flood and compress-back (to put gas back into solution by flooding with high pressure drop and increased backpressure) in an attempt to return to a  $S_{wi}$  condition. The data indicates that after this step, residual gas saturation was 0.08.

Trajectory 1 brine, oil, and gas relative permeability versus saturation results are shown in Figures 6 through 8. Subsets of the trajectory are denoted by different symbols and legend labels. After the initial saturation reversal when three-phase flow was initiated, for the most part, brine relative permeability versus brine saturation follows the (D2, I2, Ø) trend. Since  $S_w$  was near residual for most of the three-phase flow measurements, oil relative permeabilities are mostly on the two-phase gas-oil trend. For (D2, D1, I1), gas relative permeabilities follow the (R, D1, I1) trend, but for (I2, D1, D1) and subsequent cycles, gas relative permeabilities follow the (I1, Ø, D1) trend.

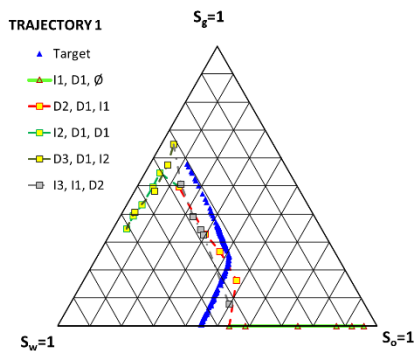


Figure 5 Saturation Trajectory 1.

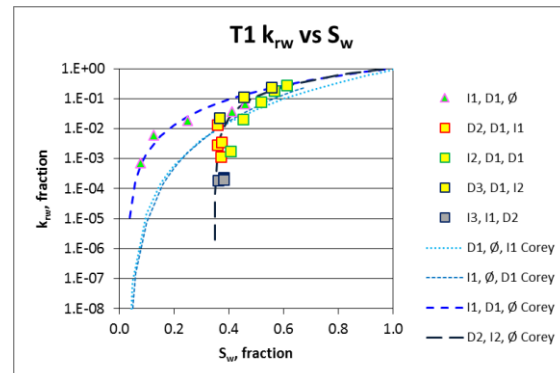


Figure 6  $k_{rw}$  versus  $S_w$ , Trajectory 1.

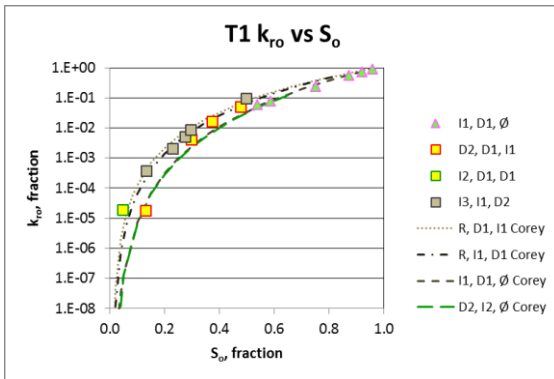


Figure 7  $k_{ro}$  versus  $S_o$ , Trajectory 1.

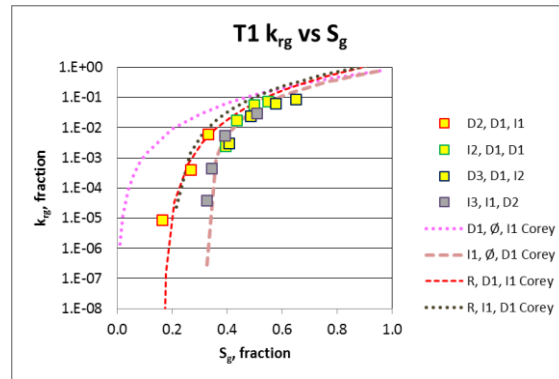


Figure 8  $k_{rg}$  versus  $S_g$ , Trajectory 1.

Trajectory 2 – At the start of Trajectory 2, brine saturation was 0.35. Gas saturation, as determined from the three-phase separator, was 0.08. Several steady-state oil-brine measurements were recorded with increasing brine fractional flow to increase brine saturation to 0.44. The first part of the trajectory was designed to measure three-phase relative permeabilities with brine saturation maintained close to the 0.44 starting condition while oil saturation decreased and gas saturation increased. After completing this segment of the Trajectory, near  $S_{or}$ , brine and gas injection rates were varied in steps for cycles of increasing and then decreasing brine saturation. The final segment of the test was to flood with oil and compress-back to  $S_{wi}$ .

Figure 9 shows saturations at which relative permeabilities were measured during Trajectory 2. Trajectory 2 brine, oil, and gas relative permeability versus saturation results are shown in Figures 10 through 12. Brine relative permeabilities mostly follow the (D2, I2, Ø) trend. Oil results mostly follow the (D2, I2, Ø) trend. Gas results are predominantly on the (R, D1, I1) trend.

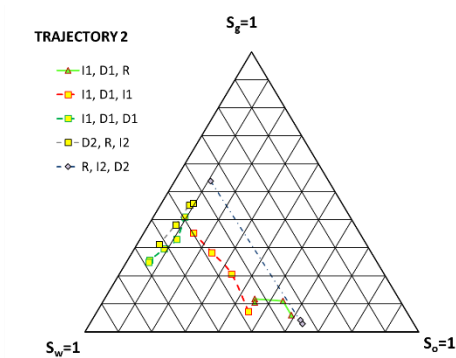


Figure 9 Saturation Trajectory 2.

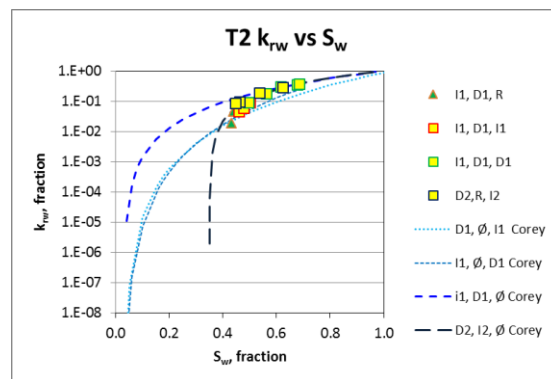


Figure 10  $k_{rw}$  versus  $S_w$ , Trajectory 2.

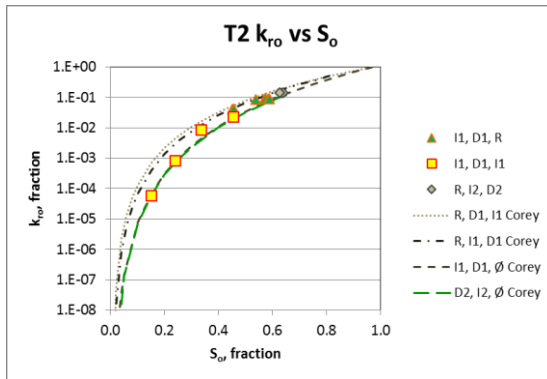


Figure 11  $k_{ro}$  versus  $S_o$ , Trajectory 2.

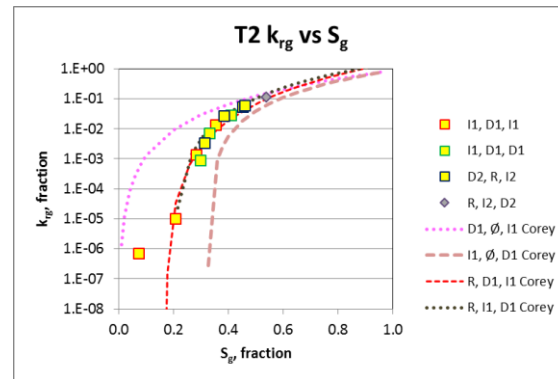


Figure 12  $k_{rg}$  versus  $S_g$ , Trajectory 2.

**Trajectory 3** - The compress-back step following the preceding saturation trajectory did not put all gas back into solution. At the start of Trajectory 3, brine saturation was 0.35. Gas saturation, as determined from the three-phase separator, was 0.07. Several steady-state oil-brine measurements were recorded with increasing brine fractional flow to increase brine saturation to 0.58. The first part of the trajectory was designed to measure three-phase relative permeabilities with increasing brine and gas saturations and decreasing oil saturation. After completing this segment of the Trajectory, near  $S_{or}$ , brine and gas injection rates were varied in steps for cycles of increasing and then decreasing brine saturation. The final segment of the test was to flood with oil and compress-back to  $S_{wi}$ . During this step, separator volumes indicate that all gas was put back into solution. The next test, Trajectory 4, was a waterflood without gas injection.

Figure 13 shows saturations at which relative permeabilities were measured during Trajectory 3. Trajectory 3 brine, oil, and gas relative permeability versus saturation results are shown in Figures 14 through 16. Brine results are mostly on the (D2, I2, Ø) trend, although saturations are in the range where (I1, D1, Ø) and (D2, I2, Ø) trends overlap. Oil results are mostly on the (D2, I2, Ø) trend. Gas results are between (D1, Ø, I1) and (R, D1, I1) trends, perhaps because for most of the test, gas saturation was increasing and oil saturation was low to moderate.

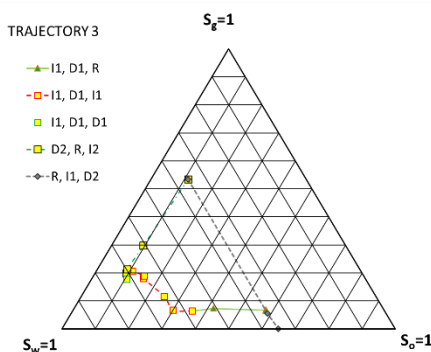


Figure 13 Saturation Trajectory 3.

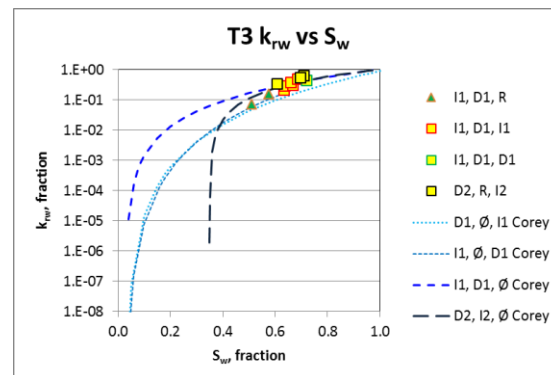
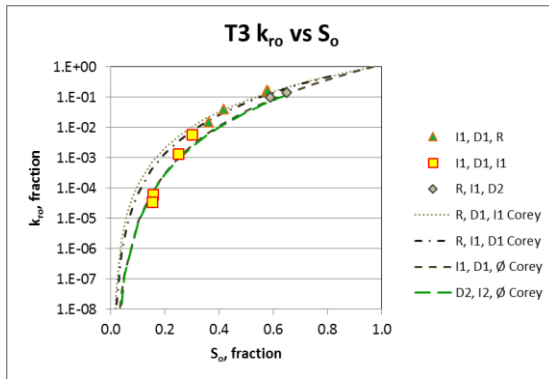
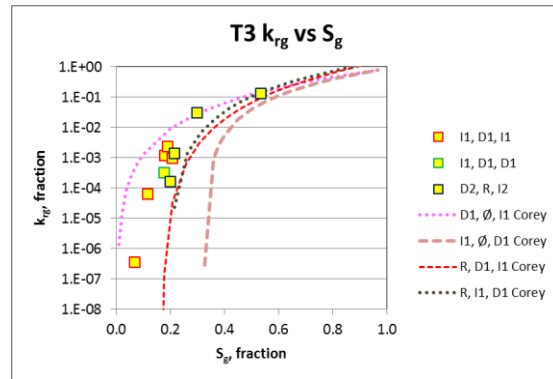


Figure 14  $k_{rw}$  versus  $S_w$ , Trajectory 3.

Figure 15  $k_{ro}$  versus  $S_o$ , Trajectory 3.Figure 16  $k_{rg}$  versus  $S_g$ , Trajectory 3.

Figures 8, 12, and 16 show that gas relative permeability in this three-phase flow system is influenced by saturation history and all three flowing phases. To estimate three-phase relative permeabilities from two-phase relative permeability functions, gas-brine as well as oil-brine and gas-oil functions are useful.

Trapped Gas - Trapped gas saturation from two- and three-phase measurements of this investigation and from the previous work are shown in Figure 17. The plot shows trapped versus initial gas saturation from measures before and after the first WAG cycle. Trapped gas saturation is lower when less gas is initially put into the pore system.

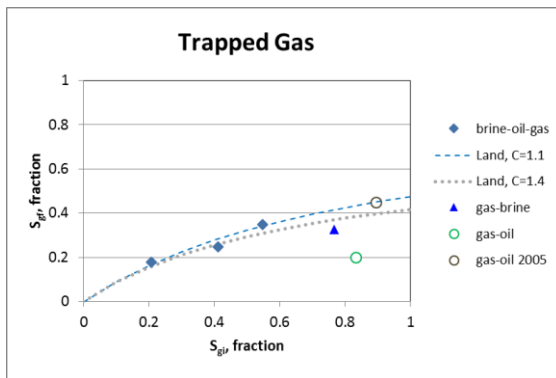


Figure 17 Trapped gas versus initial gas saturation.

## CONCLUSIONS

- Sufficient resolution was achieved to reveal saturation-history-dependent hysteresis trends.
- Trapped brine saturation was approximately 0.35 (fraction of pore volume). After increasing  $S_w$  above 0.35 during the first cycle of increasing brine saturation, brine saturation did not reduce below 0.35 during subsequent saturation cycles.
- Oil relative permeabilities with three phase flow for the most part were similar to those for two-phase oil-brine flow.
- The gas phase exhibited the greatest amount of hysteresis.

- Two-phase gas-brine curves, in addition to gas-oil curves, are useful for understanding gas relative permeability versus gas saturation in this three-phase system.
- Trapped gas saturation for the most part followed a Land trend, with trapped gas saturation increasing with increasing initial gas saturation.
- Part of the challenge in designing three-phase flow experiments is to follow saturation paths similar to the field process under investigation. For this experimentation, saturation trajectory guidance was available from a previous displacement test. For future three-phase testing, it will be useful to follow a similar protocol of performing relatively quick displacements (gas flood after waterflood or waterflood after gas flood) to identify saturation paths to follow during subsequent three-phase steady-state flow tests.

## ACKNOWLEDGEMENTS

The authors express appreciation to ExxonMobil Upstream Research Company and Hibernia Management & Development Company Ltd. for permission to present this work.

## REFERENCES

1. Wang, F., M. Honarpour, N. Djabbarah, and F. Haynes: Characterization of Multiphase Flow Properties for Tertiary Immiscible Displacement Processes in an Oil-Wet Reservoir. Paper SCA2006-33 presented at the International Symposium of the Society of Core Analysts, Trondheim, Norway (12-16 September, 2006).
2. Lawrence, J., H. Sahoo, G. Teletzke, J. Banfield, J. Long, N. Maccallum, R. Noseworthy, and L. James: Optimization of Gas Utilization to Improve Recovery at Hibernia. SPE 165240 presented at the SPE Enhanced Recovery Conference, Kuala Lumpur, Malaysia (2-4 July 2013). (OnePetro document ID 10.2118/165240-MS).
3. Johnson, E., D. Bossler, and V. Naumann: Calculation of Relative Permeability from Displacement Experiments. Petroleum Transactions AIME, V. 216 (1959). pp. 370-372. (OnePetro document ID SPE 0123-G.)
4. Wang, F., E. Braun, J. Kuzan, N. Djabbarah, M. Honarpour, C. Chiasson, and B. Milligan: Application of Unique Methodology and Laboratory Capability for Evaluation of Hydrocarbon Recovery Processes. Paper IPTC 12418 presented at the International Petroleum Technology Conference, Kuala Lumpur, Malaysia (3-5 December 2008). (OnePetro document ID 12418-MS.)
5. Braun, E., and R. Blackwell: A Steady-State Technique for Measuring Oil-Water Relative Permeability Curves at Reservoir Conditions. Paper SPE 10155 presented at the SPE Annual Technical Conference and Exhibition, San Antonio, TX (5-7 October 1981). (OnePetro document ID 10155-MS.)
6. Jones, S. and W. Roszelle: Graphical Techniques for Determining Relative Permeability From Displacement Experiments. Journal of Petroleum Technology (May, 1978), pp. 807-817. (OnePetro document 6045-PA SPE.)